

HIGH RESOLUTION SIMULATION OF GALAXY FORMATION WITH FEEDBACK

R. J. THACKER^{1,2,3} AND H. M. P. COUCHMAN^{2,4}*Draft version December 24, 2018*

ABSTRACT

We present results from a Smoothed Particle Hydrodynamic (SPH) simulation of galaxy formation that exceeds the minimum resolution requirement suggested by Steinmetz & Muller (1993) of 3×10^4 SPH particles per galaxy. Using the multiple mass technique an effective resolution of a little over one billion particles is attained within a 48 Mpc cube. We find that even with an SPH mass resolution of $1.5 \times 10^6 M_{\odot}$ and a plausible feedback algorithm, the cooling catastrophe continues to be a problem for Einstein-de Sitter CDM cosmologies. Increasing resolution also appears to exacerbate the core-halo angular momentum transport problem.

1. INTRODUCTION

Steinmetz & Muller (1993, hereafter SM93) have shown that in SPH simulations at least 3×10^4 SPH particles are necessary to accurately follow local hydrodynamic evolution, in particular shocks and velocity fields. The simulation we discuss in this *Letter* is the first simulation of galaxy formation, we are aware of, to meet this criterion and also account for long range tidal fields. The tidal fields are incorporated by using the multiple mass technique (Porter 1985).

To date, the highest resolution studies of galaxy formation including long range tidal forces are those of Navarro and Steinmetz (1997) which used up to 5,000 gas particles per galaxy. These simulations were integrated to $z = 0$ and required over 50,000 time-steps. Although the particle number is comparatively low, the integration to $z = 0$ is a significant achievement.

The simulation presented here includes star formation and feedback using an algorithm tested in detail in Thacker & Couchman (1999, hereafter TC99). Many authors believe (*e.g.* White 1994) that feedback may solve both the cooling catastrophe (White & Frenk 1991) and the associated problem of core-halo angular momentum (AM) transport (Navarro & Benz 1991). The morphological results for objects in this simulation are of great interest since we are able to probe smaller mass scales than previous investigations. This is particularly relevant in simulations with feedback since lower mass halos are more susceptible to perturbations produced by feedback.

2. ALGORITHM AND INITIAL CONDITIONS

The Bond & Efstathiou (1984) CDM power spectrum was used to assign curvature perturbations in an Einstein-de Sitter universe, with cosmological parameters $\Omega_b = 0.1$, $\Omega_{CDM} = 0.9$, $h = 0.5$, shape parameter $\Gamma = 0.41$ and normalization $\sigma_8 = 0.6$. The perturbations were assigned to a low resolution 100^3 dark-matter-only simulation of comoving width 48 Mpc, at a redshift of $z = 67$. The simulation was evolved to $z = 1$ using the adaptive P³M algorithm of Couchman (1991), at which point a halo of mass 1.66×10^{12}

M_{\odot} was selected for re-simulation. The halo, which lies on a filament approximately 2 Mpc long, does not have a violent merger history at this resolution and can be categorized as a being the halo of a field galaxy.

The initial conditions of the high resolution simulation were prepared by creating four mass hierarchies in radial shells within the simulation volume. Each shell has a width half that of the previous hierarchy, and the per-particle mass scales by a factor of 8 between each level, yielding a central high resolution region 6 Mpc in comoving diameter. The mass in this region is $7.8 \times 10^{12} M_{\odot}$, and a particle number of $2 \times 523,535$ gives particle masses of $1.5 \times 10^6 M_{\odot}$ and $1.4 \times 10^7 M_{\odot}$ for gas and dark matter respectively. The minimum ‘glob’ and dark halo mass resolutions are 52 times higher, corresponding to the number of neighbors in the SPH solver. Only the high resolution region includes SPH particles, which were given an initial temperature of 1,000 K. The effective resolution of the high resolution region is 2×800^3 . The particle positions were drawn from a ‘glass’ and the same power spectrum was used to assign modes to the particle distribution although the spectrum was truncated at the Nyquist frequency of each hierarchy. In the high resolution simulation at $z = 1$ the candidate halo is represented by about 220,000 particles, half dark matter and half gas. A Plummer softening length of $\epsilon = 1.5$ kpc was chosen and the minimum SPH smoothing length was $h_{min} = 1.76$ kpc.

In TC99 it was demonstrated that the temperature smoothing (TS) algorithm produces the most significant feedback effect. However, it was also observed that the NGC 6503 prototype was more affected by feedback than was the Milky Way prototype. Hence, given the higher resolution in this simulation, the energy smoothing (ESa) algorithm was adopted. The ESa algorithm smooths 5×10^{15} erg g⁻¹ of feedback energy over the neighbor particles of an SPH particle after a star formation event and allows this energy to persist for a time $t^* = 5$ Myr. Given the higher densities resolved in the simulation the Schmidt Law SFR normalization was reduced by 30% compared to the low resolution runs in TC99. A self-gravity criterion, also pre-

¹Theoretical Physics Institute, Department of Physics, University of Alberta, Edmonton, Alberta, T6G 2J1, Canada²Department of Physics and Astronomy, University of Western Ontario, London, Ontario, N6A 3K7, Canada.³Current address: Department of Astronomy, University of California at Berkeley, Berkeley, CA, 94720.⁴Current address: Department of Physics and Astronomy, McMaster University, 1280 Main St. West, Hamilton, Ontario, L8S 4M1, Canada.

vents star formation in regions where $\rho_b < 0.4 \rho_{DM}$.

3. RESULTS

It was not possible to integrate the simulation beyond $z = 2.16$ due to inefficiencies developed in the SPH algorithm as a result of the fixed minimum smoothing length employed. Integration to this redshift required 4,100 timesteps; approximately 37,000 would be required to $z = 0$. By $z = 2.16$ 40,777 star particles had been created (4% of the initial gas mass) and $r_{200} = 75$ kpc.

The structure and evolution of the gas in the simulation is depicted in figure 4. Three notable stages of evolution are evident: (i) by $z = 10$, five gas cores have formed with masses between $10^8 M_\odot$ and $6 \times 10^8 M_\odot$ and the associated dark halo masses are between $10^9 M_\odot$ and $5 \times 10^9 M_\odot$. A small fraction of the gas has been shocked to temperatures greater than 5,000 K, but otherwise adiabatic cooling due to expansion dominates; (ii) by $z = 5$, well over 100 dark matter halos and globes are resolved. The largest dark matter halo at this epoch has a mass of $5 \times 10^{10} M_\odot$ and the associated globe $5 \times 10^9 M_\odot$. Between $z = 3$ and $z = 5$, a large fraction of halos merge and it becomes clear that accretion on the central object is dominated by collapse along a filament in the z -direction. The hot gas halo begins developing at this epoch; (iii) by $z = 2.16$, the hot halo has evolved significantly and has a central temperature close to 10^6 K (see section 3.5). The largest dark matter halo has a mass of $6 \times 10^{11} M_\odot$, while the largest globe has a mass of $6 \times 10^{10} M_\odot$.

3.1. Morphology and the effect of feedback

In our low resolution studies (TC99) disks form a very dense gas core, with a spatial extent smaller than $0.1h_{min}$, in nearly all simulations, the exception being the highly energetic temperature smoothing feedback. There is a clear trend toward higher specific angular momenta in the gas compared to dark matter with increased feedback. However, the effect is small when compared to that needed to produce observed spiral galaxy characteristics (Fall 1983). Increasing feedback, in an attempt to unbind the dense gas cores, lead to hot halo gas being unable to cool within a Hubble time, thus rendering it unavailable for disk formation.

The higher resolution in this simulation, in combination with hierarchical clustering, leads to the the gas overcoming the self-gravity criterion, and hence forming stars, at an earlier epoch ($z = 5$) than in the simulations of TC99 ($z = 4$). Note that the 1.5 kpc resolution allows for density values that are 20 times higher than the simulations in TC99.

The dwarf systems formed here did not have the tight central gas core, observed in the lower resolution runs (TC99). The two largest dwarf systems contained over 30,000 and 20,000 gas particles respectively, before merging together at $z = 2.16$. Visualization of the dwarfs shows that feedback causes small pockets of hot gas which remain static until the region reaches the end of the feedback period at which point the gas cools rapidly. There is little evidence for ‘blow-out’.

In figure 1, the distribution of dark matter, gas and stars at $z = 2.16$ is shown. The dark matter exhibits overmerging, which should be expected, given that the gravitational force is only resolved to $0.02 r_{200}$. The dark matter

is comparatively featureless while the gas shows a number of dense cores. The results of Moore *et al.* (1998) suggest that to avoid overmerging, a force resolution of $0.002 r_{200}$ is necessary, *i.e.* ten times smaller than that used here.

The high mass resolution in the simulation allows us to resolve tidal tails extremely well. The viscosity of gas tends to accentuate the stripping effect, with collisionless matter being much less susceptible. An examination of the final state, shown in figure 1, shows that the bulk of the gas objects merging with the central core are tidally stripped as they merge. The largest dwarf system develops a ring feature because an infalling satellite becomes phase-wrapped as it accretes.

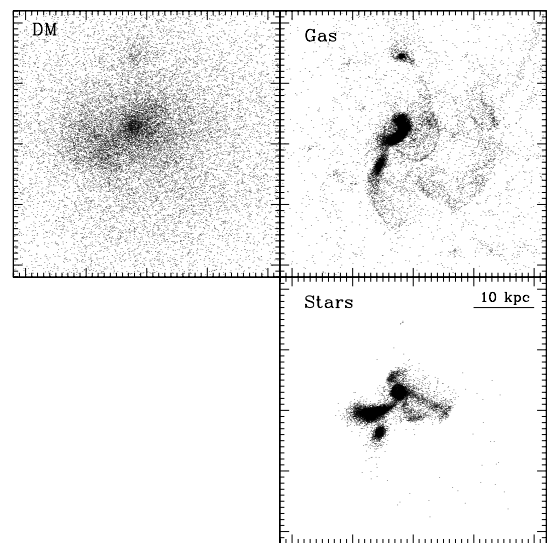


FIG. 1.—Z-projection of the dark matter, gas and stellar distributions in the main halo at $z = 2.16$. Overmerging is apparent in the dark matter and it is not possible to associate halos directly with the stellar and gaseous features.

3.2. Angular momenta of the dwarfs and main halo

To analyze the growth of the specific angular momentum, \mathbf{L} , in the two largest dwarf systems, the z -component of \mathbf{L} was compared to the expected value of a flattened rotating disk of radius R and circular velocity v_c . For a disk system with radial orbits $L_z = Rv_c$. The analysis was performed at $z = 2.2$ since the dwarfs later coalesce. For both of the systems, most of the gas and star particles have L_z values marginally under the Rv_c prediction, but do seem to follow the shape of the predicted curve reasonably well. This suggests that both of the disks have not yet lost a significant amount of angular momentum due to bar formation, although this is likely to occur. Note that the two dwarfs have well-defined disks, albeit with a comparatively low aspect ratio since the disk thickness is about 1 kpc, while the diameter is about 4 kpc (which is smaller than $4h_{min}$). Analysis of the $X_2(R)$ (Toomre 1981) data show that both disks achieve stability at around a radius of 2 kpc, which must be considered sub-resolution.

The same L_z analysis was applied to the baryon condensation in the main halo at $z = 2.16$. Although no clear

disk is yet visible, visualization shows that a number of in-falling systems are orbiting in a similar plane. Provided that these systems contribute the largest fraction of the orbital component of \mathbf{L} to the main halo, the dominant angular momentum component should be perpendicular to this plane. The data show that almost all the in-falling matter, picked out in the horizontal plane perpendicular to L_z , has lost a significant proportion of angular momentum relative to the Rv_c prediction. Since no disk has formed, all of this angular momentum loss must be due to the core-halo transport mechanism. This result appears to show that at higher resolution the angular momentum loss is greater. However, caution should be emphasized in interpreting this result: if the selected matter just happens to be passing through the plane then its \mathbf{L} vector will not align well with that of the entire system and hence the L_z analysis will overestimate the

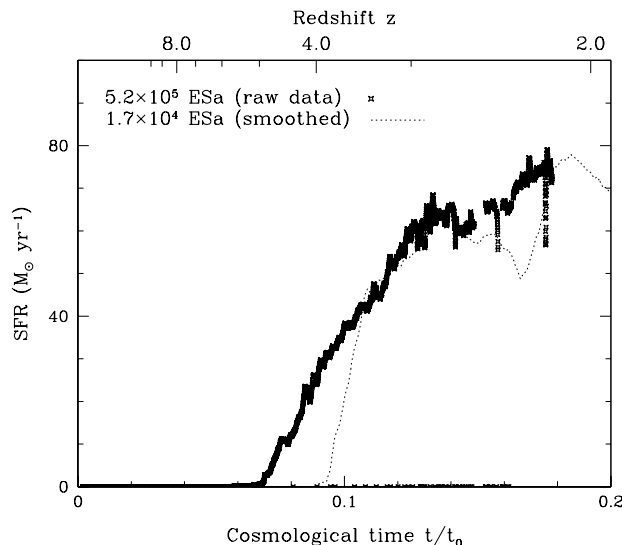


FIG. 2.—SFR integrated over the entire high resolution region. The higher mass resolution present in the simulation leads to a smoother SFR than the low resolution data (the smoothed version is shown for comparison). Points along the bottom of the plot are from code restarts and the small gap in the data is due to a log file being accidentally erased.

loss of angular momentum.

At $z = 2.16$, the largest part of the specific angular momentum within r_{200} is carried by one system very close to r_{200} . Calculation of $|\mathbf{L}|$ for the dark matter, gas cores and gas halo shows that all the values lies within a factor of two. However, recalculating these values within $r_{200}/2$, *i.e.* removing the contribution from $r \sim r_{200}$, shows markedly different results: the ratio of $|\mathbf{L}|$ of the stars to dark matter is 0.19, compared to values in the range 0.1 to 0.15 for the low resolution simulations at $z = 1$ at r_{200} in TC99. Hence the angular momentum loss in the core region is occurring earlier in this high resolution simulation.

3.3. Halo and glob mass multiplicity functions

Three redshifts were selected for analysis, namely $z = 10, 5, 2.16$. To identify halos the ‘friends of friends’ group-finding algorithm was employed. The linking length for dark matter was $r_{DM} = 0.15d$ while for the baryons it was $r_{bary} = 0.11d, 0.06d, 0.03d$ respectively for the differ-

ent red-shifts, where d is the average inter-particle spacing. The cumulative mass multiplicity functions for the dark matter and baryons are fit well by $N(< M) \propto M^{-1}$. This is shallower than the observed M^{-2} power law in Evrard *et al.* (1994), but is in close agreement with the results of Ghigna *et al.* (1999) who derive a (non-cumulative) mass multiplicity function with power law slope $dN(M)/dM \propto M^{-1.9}$ in a galaxy cluster simulation. Note, our results, and those of Ghigna *et al.*, are measured close to a density peak and are thus biased. Further, the tilt in the power law cannot be due to feedback blowing apart small baryon cores since both the dark matter and the baryons exhibit a similar slope. There is noticeably more evolution in the globs between $z = 5$ and $z = 2.16$ than there is for the dark matter halos, which is probably related to the Rees-Ostriker (1977) cooling criterion: prior to this epoch globs have not been able to cool.

3.4. Star formation rate

Although gas cores are beginning to form at $z = 10$, none of them overcomes the self-gravity criterion until $z = 5$ at which point star formation begins. The higher resolution in this simulation leads to an integrated SFR that is less burst-like than in the low resolution results of TC99. The gradient of the SFR versus time is shallower than the lower resolution runs since the SFR normalization is lower. As is shown in the plot of SFR versus time in figure 2, the peak SFR is reached at $z = 2.18$ and is $80 M_\odot \text{ yr}^{-1}$. A linear scaling of the peak value suggests an SFR of over $100 M_\odot \text{ yr}^{-1}$ would be attained if the low resolution SFR normalization from TC99 had been kept. The formation of the first star particles, and hence the first feedback events, occurred at $z = 3.4$ which is only slightly earlier than the low resolution runs ($z = 3.0$). This is due to the lower SFR normalization. Since there is no sudden drop in the SFR following the first feedback events, energy smoothing does not have a significant effect on the SFR at this resolution (as compared to the results found in the low resolution temperature smoothing, and single particle feedback experiments).

3.5. Halo properties

Although the center of the dark halo is not completely relaxed at $z = 2.16$ (the dwarfs are merging) it is still interesting to plot the radial density profile of the system since there is much interest in the shape of halo profiles (Navarro *et al.* 1997, Moore *et al.* 1998).

The densities of the dark matter and gas are shown in figure 3. A fit of the dark matter to the Moore *et al.* profile is shown for reference and the fit is excellent. The averaged SPH density (not shown) peaks about half an order of magnitude higher than the dark matter density. The self-gravity criterion is achieved out to 4ϵ , indicating that a large fraction of the condensing gas is available for star formation.

The radial temperature profile is approximately flat, *i.e.* isothermal, with a temperature of $6 \times 10^5 \text{ K}$ out to a radius of 150 kpc (ignoring gas for which $\delta_{gas} > 2000$, which is assumed to be cold dense gas in dwarf systems). The temperature declines steeply at a radius of 250 kpc, where it falls from $2 \times 10^5 \text{ K}$ to 10^4 K . The sound crossing time is 0.03 Gyr so the hot gas distribution has had time to

relax. At the center of the halo the cooling times are close to 10 Gyr, so cooling has little effect on the profile. The full three dimensional velocity dispersion for the dark matter within r_{200} was found to be 163 km s^{-1} . The average temperature for all of the gas within r_{200} was $2.4 \times 10^5 \text{ K}$, while for the hot halo it was $6.4 \times 10^5 \text{ K}$. This leads to isothermal β parameters of $\beta_{\text{all}}=1.89$ and $\beta_{\text{halo}}=0.73$. The value for the halo gas is lower than unity which is consistent with energy input from feedback.

4. CONCLUSION

This *Letter* has presented results for a simulation with sufficient mass resolution to accurately resolve shock structures within the forming galaxy. Unfortunately, due to limitations in the simulation algorithm, it was necessary to truncate the evolution of the system at $z = 2.16$.

Principal conclusions follow:

1. The cooling catastrophe continues to be a significant problem. The dwarf galaxies, even those containing greater than 10^4 gas particles, collapsed to a size close to the gravitational softening length of the simulation. However, the dwarfs did not exhibit a very tight central concentration of gas as observed in earlier low resolution models. Even given the higher mass resolution in this simulation, ESa feedback still does not cause

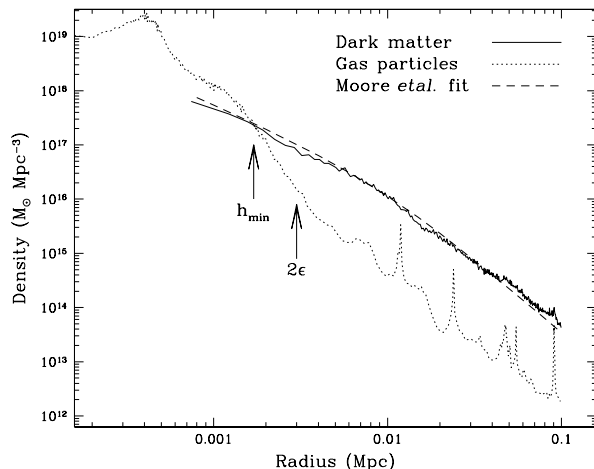


FIG. 3.—Density profiles for the dark matter and gas in the main halo. The profiles are constructed using spherical 208 particle Lagrangian bins.

strong damping of the SFR.

2. Overmerging is still observed. Including the baryons does not have any significant effect on this problem. In

the core of the main halo, a number of the baryon cores do not have an accompanying dark matter halo.

3. The core-halo angular momentum transport mechanism remains a serious problem. The star particles, which are formed from the gas cores, showed a noticeable loss of specific angular momentum relative to the dark matter at $z = 2.16$.

4. The mass multiplicity function for both the dark matter halos and globs is well fit by an M^{-1} power law. Although it is tempting to suggest this change is due to feedback reducing the number of low mass objects, this is not the case.

The higher resolution moved the onset of star formation to $z = 5$, compared to the $z \simeq 3.5$ epoch for the low resolution runs in TC99. Nonetheless $z = 5$ is still later than some of the observations suggest. For example, Chen *et al.* (1999) report the possible identification of a star-forming galaxy at $z = 6.68$. The estimated star formation rate is $70 \text{ M}_\odot \text{ yr}^{-1}$, assuming a flat, $h = 0.5$ cosmology. Given the simulation just presented, this result seems remarkable. Even though the self-gravity criterion delays star formation until comparatively late times, it is difficult to see how, with the power spectrum used, such an object could be formed. The earlier onset of star formation can be achieved by adding more resolution or by using a power spectrum with a higher normalization. However, continuing to add resolution has limits since 100 times the current mass resolution would enable the Jeans' Mass of the first objects in the CDM cosmology to be resolved, *i.e.* there is a limit to the cooling catastrophe. We note that the Lyman break galaxies, characterized by masses of a few 10^{10} M_\odot , and star formation rates of order $5-25 \text{ M}_\odot \text{ yr}^{-1}$, are quite well approximated within the simulation. The two large dwarfs could conceivably be likened to these objects.

Changes are currently being made to our simulation algorithm and we hope to evolve this simulation further with the new code. Nonetheless this simulation provides one particularly important result: even at a mass resolution of $1.5 \times 10^6 \text{ M}_\odot$, a plausible feedback algorithm still fails to prevent the cooling catastrophe.

The authors thank Jimmy Scott of SGI-Cray Canada for securing a grant of supercomputer time at the Eagan Supercomputing Center where part of this research was conducted. A grant of time on the UK-CCC server, 'COSMOS', provided by the Virgo Consortium is also acknowledged. RJT was supported by a Dissertation Fellowship from the University of Alberta while this research was conducted. HMPC thanks NSERC of Canada for financial support.

REFERENCES

Chen, H. W., Lanzetta, K. M., & Pascarelle, S., 1999, *Nature*, 398, 586
 Couchman, H. M. P., 1991, *ApJ*, 368, L23
 Evrard, A. E., Summers, F. J., & Davis, M., 1994, *ApJ*, 422, 11
 Fall, S. M., 1983, in *Internal Kinematics and Dynamics of Galaxies*, ed. E. Athanassoula, (Reidel), p. 391
 Ghigna, S., Moore, B., Governato, F., Lake, G., Quinn, T., & Stadel, J., 1999, *astro-ph/9910166*
 Moore, B., Governato, F., Quinn, T., Stadel, J., & Lake, G., 1998, *ApJL*, 499, L5
 Navarro J., & Benz, W., 1991, *ApJ*, 380, 320
 Navarro J., & Steinmetz, M., 1997, *ApJ*, 478, 13
 Navarro, J. F., Frenk, C. S., & White, S. D. M., 1997, *ApJ*, 490, 493
 Nusser, A., & Sheth, R. K., 1999, *MNRAS*, 303, 685
 Porter, D., 1985, PhD Thesis, University of California, at Berkeley.
 Rees, M. J., & Ostriker, J. P., 1977, *MNRAS*, 179, 541
 Steinmetz, S., & Muller, E., 1993, *A&A*, 268, 391
 Thacker, R. J., & Couchman, H. M. P., submitted to *ApJ*
 Toomre, A., 1981, in *The Structure and Evolution of Normal Galaxies*, eds. S. M. Fall & D. Lyden-Bell, (Cambridge: Cambridge Univ. Press), p. 111
 White, S. D. M., 1994, *Les Houches Lectures*, *astro-ph/9410043*
 White, S. D. M., & Frenk, C. S., 1991, *ApJ*, 379, 52

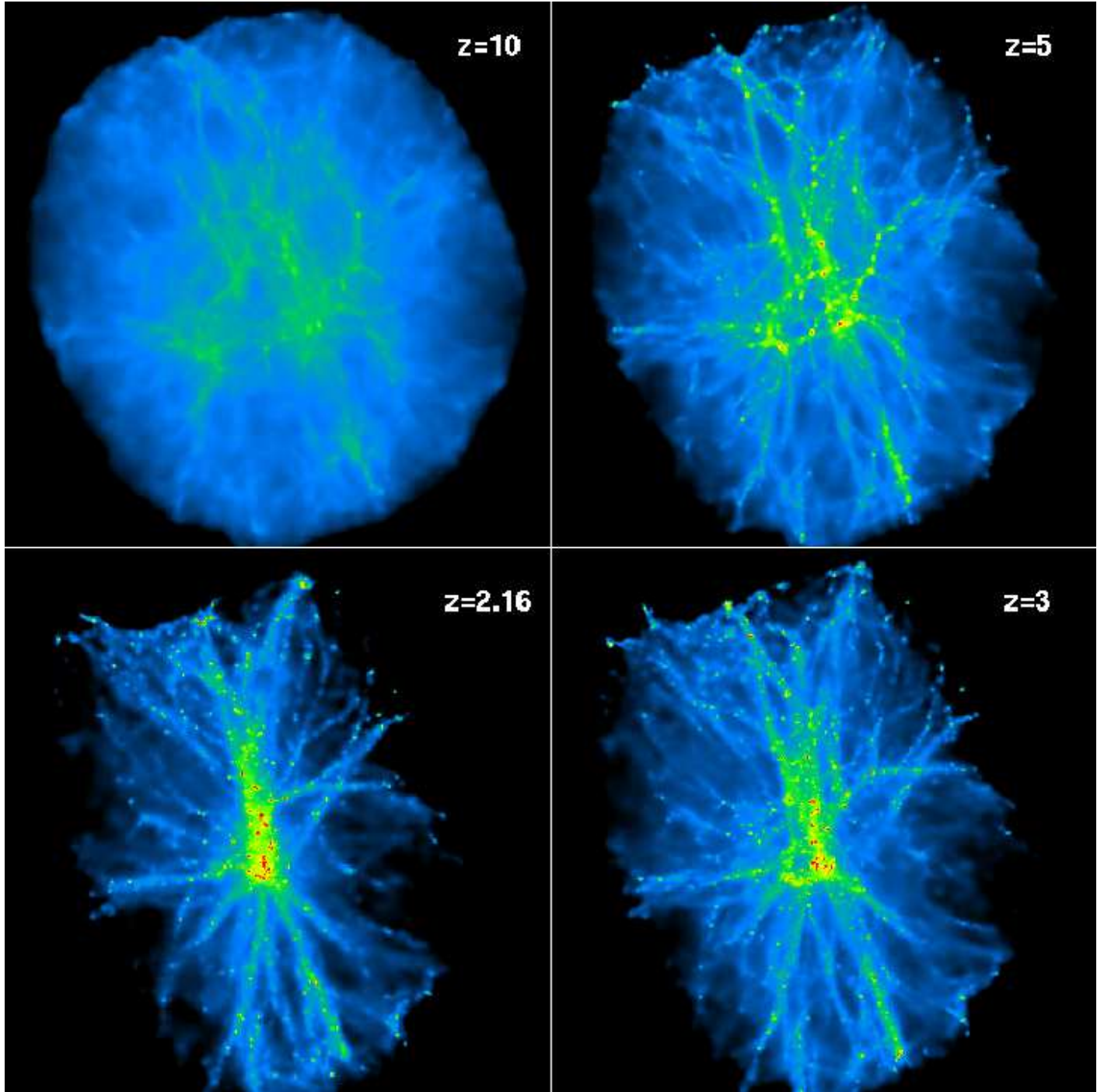


FIG. 4.—4-panel plot showing the evolution of the comoving density from $z = 10$ to the final epoch $z = 2.16$. The SPH data is smoothed onto a grid with spacing h_{min} , thus the grids are a realistic representation of the resolution. In physical coordinates the top left panel would be 3.48 times smaller than the bottom left. The color scheme runs from $10^{18} n_B \text{ cm}^{-3}$ (blue) to $10^{21} n_B \text{ cm}^{-3}$ (red). The filamentary structure is already forming at $z = 10$ and by $z = 5$ the first halos have reached sufficient density to form stars. Evolution from $z = 3$ to $z = 2.16$ is dominated by collapse along the x-direction. Note that the z-projection looks directly along a filament and thus over-emphasizes the collapse.